Nonlinear Dynamics of a Sigma-Delta modulator with Integrator Leakage

Emer Condon[†], Alexey Teplinsky * and Orla Feely[‡]

†Dept. of Electronic and Electrical Engineering,University College Dublin
Belfield, Dublin 4, Ireland.
*Institute of Mathematics, Natl. Acad. Sc. of Ukraine,
3 Tereshchenkivska St, Kyiv 01601, Ukraine.

Email: emer.condon@ee.ucd.ie, orla.feely@ucd.ie, teplinsky@imath.kiev.ua

Abstract–The behaviour of the first-order Sigma-Delta ($\Sigma\Delta$) modulator with integrator leakage, a common circuit imperfection is investigated using methods of nonlinear dynamics. Both continuous and discrete time modulators are considered. The results found provide information about the size of the internal variables in steady state, and also about the specific behaviour of those variables.

1. Introduction

Sigma-delta ($\Sigma\Delta$) modulators are widely used for analogue-to-digital and digital-to-analogue conversion in both discrete-time and continuous-time implementations [1]. A $\Sigma\Delta$ modulator is an example of a nonlinear system, the nonlinearity being introduced by the presence of the quantiser. In [2] we applied results of our work on driven interval shifts to explain the steady-state dynamics of the first-order ideal discrete-time $\Sigma\Delta$ modulator whose input is a sampled periodic signal. In [3] the $\Sigma\Delta$ modulator with integrator leakage, a common circuit imperfection, was explored. In particular, it was found that under certain conditions the trajectories tend in the limit to lie on two continuous curves.

In this paper, an explicit formula for these curves with any periodic input is determined. We will begin by reviewing some of our previous results. In section 3, the new algorithm is presented and then applied to the case of sinusoidal input and a triangular wave input. Finally, the effect of the integrator leakage on the thickness of the limit set [2] is examined.

2. The Sigma-Delta Modulator

2.1. $\Sigma\Delta$ Modulators

Fig. 1 shows the basic first-order $\Sigma\Delta$ modulator in both (a) discrete- and (b) continuous-time implementations. Ideal discrete-time and continuous-time modulators are obtained by setting $p = 1$ and $a = 0$ respectively.
The system in Fig.1 (a) is modelled by the piecewise-linear equation

$$u_{n+1} = pu_n + x_{n+1} - \mathrm{sgn}(u_n) \tag{1}$$

where $\mathrm{sgn}(u_n) = 1$ when $u_n \geq 0$ and -1 when $u_n < 0$.

In the ideal continuous-time sigma-delta modulator, i.e. the system of Fig. 1(b) with $a = 0$, the quantizer samples the signal $u(t)$ with period T. This system is described by the equation:

$$\frac{du(t)}{dt} = x(t) - \mathrm{sgn}(u(nT)) \quad \text{for } nT \leq t < (n+1)T$$

Integrating between nT and $(n+1)T$ and scaling by T gives the equation

$$\bar{u}_{n+1} = \bar{u}_n + \bar{x}_{n+1} - \mathrm{sgn}(\bar{u}_n) \tag{2}$$

where

$$\bar{x}_{n+1} = \frac{1}{T}\int_{nT}^{(n+1)T} x(t)dt \quad \text{and} \quad \bar{u}_n = \frac{u(nT)}{T}$$

Eq. (2) is of the form (1), and so our analysis of the dynamics of (1) will apply to both the discrete- and continuous-time modulators.

The non-ideal continuous-time system can also be modelled by an equation of this form, proceeding as before by integrating over a time-step and changing variables, with $p = e^{-aT}$.
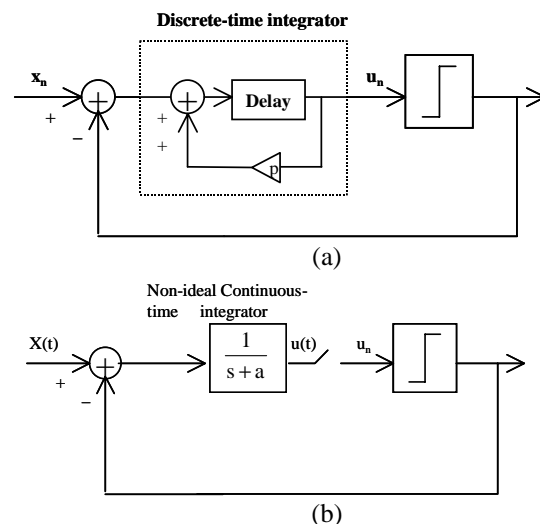

(a)

(b)

Figure 1 (a) Discrete-time first-order $\Sigma\Delta$ modulator. (b) Continuous-time first-order $\Sigma\Delta$ modulator.

Eq. (1) can be converted to autonomous form, when x_n is the sampled version of a periodic signal f of frequency ω, and this gives the 2D mapping:

$$F : \begin{pmatrix} \theta \\ u \end{pmatrix} \rightarrow \begin{pmatrix} \theta + \omega \bmod 2\pi \\ pu + f(\theta + \omega) - \operatorname{sgn} u \end{pmatrix} \qquad (3)$$

2.2 Nonlinear Dynamics of Ideal ($\Sigma\Delta$) Modulators.

The limit behaviour of the mapping in (3) with p=1 was studied in [2]. In this case, it was found that:

If $\quad \dfrac{1}{2\pi}\left|\displaystyle\int_0^{2\pi} f(\theta)d\theta\right| < 1 \quad$ then there exists a belt

$B = \{(\theta, u)\,|\,L(\theta) \le u < U(\theta)\}$ of constant thickness $U(\theta) - L(\theta) = 2$ that absorbs all trajectories of (3) and is invariant. If $|f(\theta)| < 1$ for all θ, the belt is bounded by the curves

$$C_1^+ = f(\theta) + 1 \text{ and } C_1^- = f(\theta) - 1 \qquad (4)$$

Otherwise the boundaries consist of a finite number of the critical curves [4] given by

$$\begin{aligned} & C_1^+, \ C_1^-, \\ & C_n^+ = F(C_{n-1}^+) \text{ and } C_n^- = F(C_{n-1}^-) \text{ for } n \ge 2. \end{aligned} \qquad (5)$$

In [3], the effect of including integrator leakage into the map in (3), i.e. $p < 1$ case, on the dynamics was investigated. The dynamics were found to be qualitatively different from those of the ideal case. In this paper, the limit behaviour of this mapping for $p < 1$ is investigated further.

## 3. Nonlinear Dynamics of Non-Ideal ($\Sigma\Delta$) Modulator.

Firstly, it was found that the belt $B_1 = \{(\theta, u)\,|\,f(\theta) - 1 \le u < f(\theta) + 1\}$ bounded by C_1^+ and C_1^- from (4) is invariant with respect to the mapping (3) under the following condition:
$$|f(\theta)| < 2/p - 1 \text{ for all } \theta$$
However, the belt B_1 is no longer mapped onto itself by F when $p < 1$. For values of θ such that $|f(\theta)| < 1$, its section $B_1(\theta) = [f(\theta) - 1, f(\theta) + 1)$ maps to two intervals of combined length $2p$ separated by a gap of length $2 - 2p$. For values of θ such that $1 < |f(\theta)| < 2/p - 1$, $B_1(\theta)$ does not contain 0 and thus maps to a single interval of length $2p$. It is easy to see that this pattern continues, and after k iterations the interval $B_1(\theta)$ maps to m interval components within $B_1(\theta + k\omega)$, for some $1 \le m \le k$, of combined length $2p^k$ (on every step, if an iterate of $B_1(\theta)$ contains 0, then its image gets one extra component). Since $p < 1$, it is clear that this combined length tends to 0 as the number of iterations tends to infinity, and so the limit set (which is rigorously defined as the intersection of the closures of consecutive iterates of the belt) where trajectories reside in steady state has measure zero within the belt B_1. It is also clear that the boundary points of the interval components at any stage of the iteration process lie on the critical curves C_n^+ and C_n^- defined in (5).

3.1 The Limiting Curves.

The main result in [3] which is of interest in this paper is that for the case of $|pf(\theta) + f(\theta + \omega)| \le 1 - p$ for all θ, the iteration of B_1 produces in the limit two continuous curves. A trajectory of (3) is shown in steady-state in Fig. 2(b). Note how the trajectory lies on the curves from Fig. 2(b). The dynamics are quite straightforward: with each iteration the trajectory moves to the right by a distance ω, bouncing between the curves. In this section, an explicit formula for these limit curves is determined.
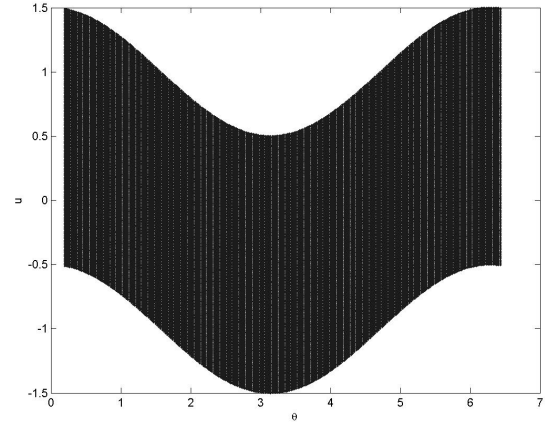
(a)
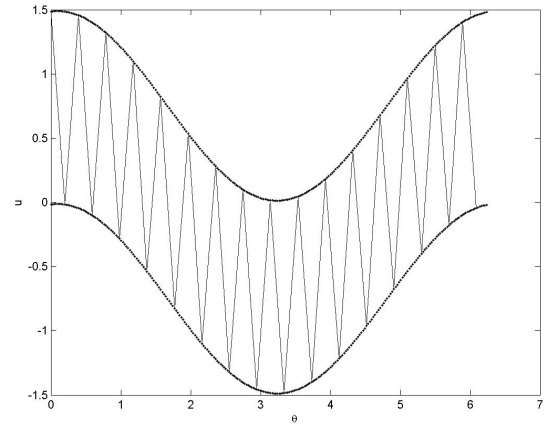
(b)

Figure 2 (a) The belt B_1 bounded by $A\cos\theta \pm 1$ (b) The limit obtained as the number of iterations of B_1 tends to infinity. $A = 0.5$, $p = 0.332$ and $\omega = \pi/32$. A trajectory of (3) is plotted jumping between the limit curves.

3.1.1 The equations of the limit curves

Consider any periodic input $f(\theta)$ which can be expressed in terms of its Fourier series as follows:

$$f(\theta) = k_f + \sum_{n=1}^{\infty} a_{f_n} \cos(n\theta) + \sum_{n=1}^{\infty} b_{f_n} \sin(n\theta).$$

Now the continuous curves on which the trajectory lies can be described as:

$$C_U(\theta) = k_U + \sum_{n=1}^{\infty} a_{U_n} \cos(n\theta) + \sum_{n=1}^{\infty} b_{U_n} \sin(n\theta)$$

and $C_L(\theta) = k_L + \sum_{n=1}^{\infty} a_{L_n} \cos(n\theta) + \sum_{n=1}^{\infty} b_{L_n} \sin(n\theta)$.

We will proceed by analysing the case of $C_U(\theta)$.

Consider the upper limit curve:

If $C_U(\theta) = k_U + \sum_{n=1}^{\infty} a_{U_n} \cos(n\theta) + \sum_{n=1}^{\infty} b_{U_n} \sin(n\theta)$

then

$$C_U(\theta + 2\omega) = k_U + \sum_{n=1}^{\infty} a_{U_n} \cos(n\theta + 2n\omega) + \sum_{n=1}^{\infty} b_{U_n} \sin(n\theta + 2n\omega)$$

Using the following trigonometric identities
$$\sin(\theta + \omega) = \cos\theta \sin\omega + \sin\theta \cos\omega$$
$$\cos(\theta + \omega) = \cos\theta \cos\omega - \sin\theta \sin\omega$$

Then

$$C_U(\theta + 2\omega) =$$
$$k_U + \sum_{n=1}^{\infty} (a_{U_n} \cos(2n\omega) + b_{U_n} \sin(2n\omega)) \cos(n\theta) \quad (6)$$
$$+ \sum_{n=1}^{\infty} (b_{U_n} \cos(2n\omega) - a_{U_n} \sin(2n\omega)) \sin(n\theta)$$

From (3),
$$C_U(\theta + 2\omega) = pC_U(\theta + \omega) + f(\theta + 2\omega) + 1$$

which in turn gives
$$C_U(\theta + 2\omega) = p^2 C_U(\theta) + pf(\theta + \omega) + f(\theta + 2\omega) - p + 1$$

Now substituting for $f(\theta)$ and $C_U(\theta)$ gives the following:

$$C_U(\theta + 2\omega) = p^2 \left(k_U + \sum_{n=1}^{\infty} a_{U_n} \cos(n\theta) + \sum_{n=1}^{\infty} b_{U_n} \sin(n\theta) \right) +$$
$$p \left(k_f + \sum_{n=1}^{\infty} a_{f_n} \cos(n\theta + n\omega) + \sum_{n=1}^{\infty} b_f \sin(n\theta + n\omega) \right) + k_f +$$
$$\sum_{n=1}^{\infty} a_{f_n} \cos(n\theta + 2n\omega) + \sum_{n=1}^{\infty} b_{f_n} \sin(n\theta + 2n\omega) - p + 1$$

Again using the trigonometric identities given above,

$$C_U(\theta + 2\omega) = p^2 k_U + pk_f + k_f - p + 1 +$$

$$\sum_{n=1}^{\infty} (p^2 a_{U_n} + pa_{f_n} \cos(n\omega) + pb_{U_n} \sin(n\omega) + a_{f_n} \cos(2n\omega) +$$
$$b_{f_n} \sin(2n\omega)) \cos(n\theta) +$$

$$\sum_{n=1}^{\infty} (p^2 b_{U_n} - pa_{f_n} \sin(n\omega) + pb_{U_n} \cos(n\omega) - a_{f_n} \sin(2n\omega)$$
$$+ b_{f_n} \cos(2n\omega)) \sin(n\theta)$$

$$(7)$$

Equation (6) and (8) must be equal. Firstly, the constant term k_U can be determined easily.

$$k_U = p^2 k_U + pk_f + k_f - p + 1$$

Hence, $k_U = \dfrac{pk_f + k_f - p + 1}{1 - p^2}$.

Similarly, $k_L = \dfrac{pk_f + k_f + p - 1}{1 - p^2}$

For each n, it can be seen that

$$\begin{bmatrix} \cos(2n\omega) - p^2, & \sin(2n\omega) \\ -\sin 2\omega, & \cos(2n\omega) - p^2 \end{bmatrix} \begin{bmatrix} a_{U_n} \\ b_{U_n} \end{bmatrix} =$$
$$\begin{bmatrix} pa_{f_n} \cos(n\omega) + pb_{U_n} \sin(n\omega) + a_{f_n} \cos(2n\omega) + b_{f_n} \sin(2n\omega) \\ -pa_{f_n} \sin(n\omega) - pb_{f_n} \cos(n\omega) - a_{f_n} \sin(2n\omega) + b_{f_n} \cos(2n\omega) \end{bmatrix}$$

Letting $M_n = \begin{bmatrix} \cos(2n\omega) - p^2, & \sin(2n\omega) \\ -\sin(2n\omega), & \cos(2n\omega) - p^2 \end{bmatrix}$ and

$$C_n =$$
$$\begin{bmatrix} pa_{f_n} \cos(n\omega) + pb_{f_n} \sin(n\omega) + a_{f_n} \cos(n2\omega) + b_{f_n} \sin(n2\omega) \\ -pa_{f_n} \sin(n\omega) - pb_{f_n} \cos(n\omega) - a_{f_n} \sin(n2\omega) + b_{f_n} \cos(n2\omega) \end{bmatrix}$$

Provided that $\det(M_n) \neq 0$ then

$$\begin{bmatrix} a_{U_n} \\ b_{U_n} \end{bmatrix} = M_n^{-1} C_n \quad (8)$$

Similarly, for $\begin{bmatrix} a_{L_n} \\ b_{L_n} \end{bmatrix} = M_n^{-1} C_n$.

3.2. A sinusoidal input.

Consider the case of $f(\theta) = A\cos\theta$. This is the simplest case where $k_f = 0$, $a_{f1} = A$, $a_{fn} = 0$ for $n > 1$ $b_{fn} = 0$ for all n.

Here $k_U = k_L = \dfrac{1}{1 + p}$. $M_1 = \begin{bmatrix} \cos(2\omega) - p^2, & \sin(2\omega) \\ -\sin(2\omega), & \cos(2\omega) - p^2 \end{bmatrix}$

and $C_1 = \begin{bmatrix} pA\cos(\omega) + A\cos(2\omega) \\ -pA\sin(\omega) - A\sin(2\omega) \end{bmatrix}$

Then by (8)

$$\begin{bmatrix} a_{U_1} \\ b_{U_1} \end{bmatrix} = M_1^{-1}C_1 \text{ and } \begin{bmatrix} a_{L_1} \\ b_{L_1} \end{bmatrix}, M_n = 0 \text{ and } C_n = 0 \text{ for } n > 1$$
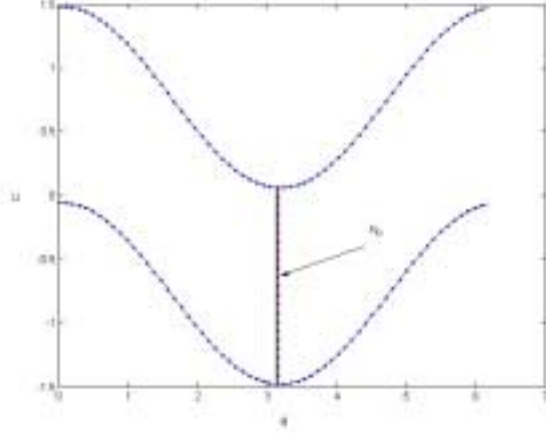

Figure 3   The continuous curves are plotted for $A = 0.5$, $p = 0.3$ and $\omega = \pi/32$. The continuous lines represent the curves found using (6). The dots are found by repeatedly iterating the process using (3). K_D represents the thickness of the limit set.

3.3. A triangle wave input.

Consider a triangular wave input which is represented by the following Fourier series [5]:

$$f(\theta) = \frac{1}{T_0} + \frac{8}{\pi^2 T_0}\left[\cos(\theta) + \frac{1}{3^2}\cos(3\theta)\dots\right]$$

Now $k_f = \frac{1}{T_0}$, $a_{f_n} = \frac{8}{\pi^2 T_0 n^2}$ for odd n and $a_{f_n} = 0$ for

even n; $b_{f_n} = 0$ for all n.

$$k_U = \frac{pk_f + k_f - p + 1}{1 - p^2}, k_L = \frac{pk_f + k_f + p - 1}{1 - p^2}$$

$$M_n = \begin{bmatrix} \cos(2n\omega) - p^2, & \sin(2n\omega) \\ -\sin(2n\omega), & \cos(2n\omega) - p^2 \end{bmatrix} \text{ for odd } n$$

$$C_n = \begin{bmatrix} pa_{f_n}\cos(n\omega) + a_{f_n}\cos(2n\omega) \\ -pa_{f_n}\sin(n\omega) - a_{f_n}\sin(2n\omega) \end{bmatrix} \text{ for odd } n.$$

$M_n = 0$ and $C_n = 0$ for even n.

Hence $\begin{bmatrix} a_{U_n} \\ b_{U_n} \end{bmatrix} = M_n^{-1}C_n$ and $\begin{bmatrix} a_{L_n} \\ b_{L_n} \end{bmatrix} = M_n^{-1}C_n$ for odd n.

4. The Thickness of the Limit Set.

In [2], the thickness of the invariant belt is constant: $U(\theta) - L(\theta) = 2$. For the mapping in (3), the thickness of the two-curve limit set can be determined using the formulae for $C_U(\theta)$ and $C_L(\theta)$ in the previous section.

Since $\begin{bmatrix} a_{U_n} \\ b_{U_n} \end{bmatrix} = \begin{bmatrix} a_{L_n} \\ b_{U_n} \end{bmatrix}$ for all n, it is easy to see:

$$K_D = C_U(\theta) - C_L(\theta) = \frac{2}{1 + p} \text{ for all } \theta.$$
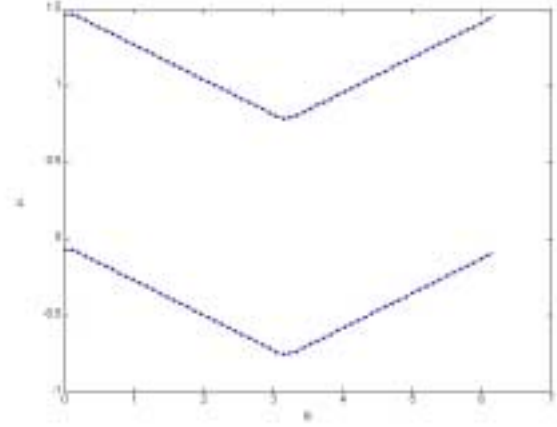
This is evident in Fig. 3.

Figure 4 The continuous curves are plotted for $k_f = 1/4$, $a_{fn} = 0.202/n^2$, $p = 0.3$ and $\omega = \pi/32$. . The continuous lines represent the curves found using (6). The dots are found by repeatedly iterating the process using (3).

5. Conclusions

In this paper, we considered the nonlinear dynamics of a map modeling discrete-and continuous-time first-order sigma-delta modulators with sampled periodic input. In particular, an explicit formula for the limiting curves and the thickness of the limit set was determined.

References

[1] S. Norsworthy, R. Schreier and G Temes, eds., *Delta-Sigma Data Converters: Theory, Design and Simulation*, IEEE Press, New York, 1997.

[2] A. Teplinsky, E. Condon and O. Feely, "Driven Interval Shift Dynamics in Sigma Delta Modulators and Phase-Locked Loops", to appear in *IEEE Trans. Circuits and Systems Part I: Fundamental Theory and Applications*.

[3] E. Condon and O. Feely, "Nonlinear dynamics of a nonideal sigma-delta modulator with periodic input." *Proceedings of the IEEE International Symposium on Circuits and Systems (ISCAS)*, 2004.

[4] C. Mira, L. Gardini, A. Barugola and J. C. Cathala, *Chaotic Dynamics in Two-Dimensional Non-Invertible Maps*, World Scientific, Singapore, 1996.

[5] E. Oran Brigham, *The Fast Fourier Transform and its Applications,* Prentice Hall Signal Processing series ,1988.